

Supplementary Methods:

RNA-seq Analysis

The preparation of whole transcriptome libraries and deep sequencing were performed by Novogene (CA, USA). To estimate gene expression level, the read counts were expressed as fragments per kilobase of exon per million (FPKM). mRNA was purified from total RNA using poly-T oligo-attached magnetic beads, further fragmented, and used as templates for cDNA generation. First strand cDNA was synthesized using random hexamer primers and reverse transcriptase. Second strand cDNA was synthesized based on the first strand with dNTP, buffer solution, DNA polymerase I and RNase H. Double-stranded cDNA was then purified using AMPure XP beads, and the second strands (containing uridines) were degraded using the USER Enzyme. Purified double-stranded cDNA was then end-repaired, a poly(A) tail added, and ligated to paired-end Illumina sequencing adaptors. cDNA fragments of 150~200bp were preferentially size-selected using AMPure XP system (Beckman Coulter, Beverly, USA) and amplified by PCR. Sequencing was performed using the Illumina HiSeq-PE150 platform. Sequence reads were aligned to the mouse genome sequence and annotated using the Ensembl project with Tophat2.¹

Nanostring nCounter miRNA Assay for miRNA Profiling

Briefly, unique DNA tags were ligated to the 3' end of each mature miRNA. After ligation, samples were cleaned to remove excess tags and hybridized to a panel of miRNA:tag-specific nCounter capture and barcoded reporter probes. Fluorescence was collected on the nCounter Digital Analyzer (NanoString Technologies) from individual

fluorescent barcodes to quantify the targeted RNA molecules present in each sample. Raw data was normalized to the top 100 expressed miRNA as determined by the NanoString nSolver software.

Histological Analysis

Five-micron paraffin sections were prepared, de-paraffinized in xylene-alcohol series, followed by rehydration in 1× phosphate buffered saline (PBS). Slides were stained with hematoxylin and eosin (H&E) to evaluate metaplasia in the corpus. Specific protein expression was identified by immunostaining. Cultured cells were fixed in -20°C acetone for 5-10min. Slides were placed in 10mM citric acid buffer (pH 6) and heated to near boiling in a water bath for 20 min for antigen retrieval, and then washed in 0.01% Triton X-100 in PBS twice, incubated for 1 hour with the serum of the animal in which the secondary antibody was raised. The slides were then incubated at 4°C overnight with SLFN12L (1:100, #NBP1-91060, NOVUS), CD44 v10-e16 (1:10,000, #CAC-LKG-M002, Cosmo Bio), or lectin GSII from *Griffonia simplicifolia* (1:1000, Alexa Fluor™ 488 conjugate, #L21415, Thermo Fisher), and then the Alexa Fluor–conjugated secondary antibody (1:500, Molecular Probes, Invitrogen) at room temperature for 30 min. The ProLong Gold Antifade reagent with DAPI (Life Technologies) was added to the slide prior to the coverslip. Species-matched secondary antibodies without primary antibodies were used as the negative controls. Immunofluorescence was visualized using a Nikon Eclipse E800 microscope.

Flow Cytometry

Stomach was minced, then incubated in 20 ml of collagenase solution (1.5 mg/ml Type VIII Collagenase) dissolved in pre-warmed CMF HBSS/FBS with 40 µg/ml of DNase I for digestion at 200 rpm for 20 min at 37°C. After passing through the 100 µm cell strainer and centrifuging at 1500 rpm for 5 min at 4°C, the cell pellet was re-suspended in PBS containing 5% BSA. Cell suspensions were blocked with purified rat anti-mouse DC16/CD32 mouse Fc block (BD Biosciences, San Diego, CA) at 4°C for 5 min, prior to incubating with CD8a-APC (#17-0081-8, Thermo Fisher) and CD45-FITC (#50-163-420, Thermo Fisher). The cells were analyzed using a BD FACSCanto II system (BD Biosciences).

MTT Cell Proliferation Assay

The MTT assay kit (Cayman) was used to detect the effect of MIR130b on cell proliferation. Briefly, cells (2×10^5 cells/ml) transfected with MIR130b mimic or antisense were seeded onto 96-well plates and cultured for 72h. Four hours prior to assaying, the cells were mixed with MTT reagent and returned to the incubator to allow the cells to reduce the MTT reagent for 4 h. The formazan produced by the cells appeared as purple/black dots in the wells. The plate was centrifuged at 400 x g for 10 min to pellet the cells and to remove the supernatant. The crystal dissolving detergent solution (100µl) was added to the wells and pipetted to mix. Sample absorbance was measured at 570nm in a 1420 microplate reader (PerkinElmer).

Western Blot Analysis

Total protein was extracted from HL-60 cells in RIPA buffer (Pierce, Rockford, IL). Nuclear and cytoplasmic proteins were extracted from the xenograft tumors using the NE-PER™ reagent kit (Thermo Fisher, 78833) following the manufacturer's protocol. Western blotting was performed with a SDS-PAGE Electrophoresis System (Invitrogen). Briefly, 20µg of protein was re-suspended in sample buffer, and then electrophoresed on a Novex 4–20% Tris-Glycine gradient gel (Invitrogen) with Tris running buffer; blotted to PVDF membrane using the iBlot Dry Blotting System (Invitrogen) according to the manufacturer's instructions. The membranes were incubated in non-fat dry milk for 1 hour at room temperature and then sequentially probed with primary antibodies against GLI1 (#PA122557, Thermo), CYLD (#4495S, Cell Signaling Technology), NFκB-p65 (#710048, Invitrogen), GAPDH (#MA5-15738, Thermo), α-Tubulin (#2144S, Cell Signaling) and human histone 3 (#9715S, Cell Signaling) overnight at 4 °C. Membranes were subsequently washed in TBST (0.1% Tween) for 30 minutes then incubated with HRP-conjugated secondary antibodies. Finally, membranes were incubated in SuperSignal™ West Pico PLUS Chemiluminescent Substrate (#34580, Thermo Scientific) and developed on x-ray film (#490001-950, GeneMate). The quantitation by ImageJ reflected the amount as a ratio of each protein band relative to the lane's loading control from 3 expts.

***Helicobacter pylori* Culture and Infection**

Helicobacter pylori (*H. pylori*, SS1 strain) was obtained from the American Type Culture Collection (ATCC) and were grown on blood agar plates prior to inoculation of sterile-filtered Brucella broth (BD, Franklin Lakes, NJ) plus 10% horse serum (Atlanta

Biologicals, Lawrenceville, GA). *H. pylori* cultures were maintained by shaking at 100 rpm in the GasPak™ EZ Campy Container System (BD Biosciences) at 37°C. The presence of *H. pylori* was verified biochemically by catalase and urease tests as well as microscopic analysis for size, shape, and motility. The cultures were pelleted at 2700 rpm at room temperature, and then re-suspended in saline. The optical density of *H. pylori* was measured and the final concentration was adjusted to 10⁸ organisms per ml of serum-free cell media.

Chromatin Immunoprecipitation Assay

The chromatin immunoprecipitation (ChIP) assay was performed using EZ Magna ChIP A/G kit (Millipore). HL-60 cells transfected with MIR130b mimic or scrambled control were treated with 1% formaldehyde and then quenched with glycine for 5 min at room temperature. Cell lysates were sonicated to shear DNA into fragments of 200 to 1000 bp using a 130W Sonic Vibracell (VCX130PB). An aliquot (5%) of the lysate was removed and used as the input, while the remaining solution was used to immunoprecipitate cross-linked protein using a NFκB p65 monoclonal antibody (#C1004, Invitrogen) overnight at 4°C. An IgG antibody was used as the negative control and RNA polymerase II (RNAPII) was used as the positive control. Protein/DNA complexes were harvested using Protein A/G agarose beads. After reverse cross-linking the complexes to free DNA, qPCR was performed using promoter-specific primers for MIR130b, IκB, NOS2. GAPDH was used as a gene not regulated by NFκB. The predicted NFκB binding sites on the MIR130b promoter were located at -229 to -239 (BS1), -474 to -484 (BS2), and -1467 to -1477 (BS3) upstream of the

transcription start site (TSS) of MIR130b as previously described². The TSS was confirmed in silico in the Santa Cruz Genome Browser (<https://genome.ucsc.edu>). The site where the RNAP2 (POLR2, RNA polymerase 2) binds is the approximate start site. The NFkB site can also be approximated using the genome browser followed by comparing the sequences to the NFkb consensus site. Moreover, some analyses of the MIR130b promoter have recently been published.^{3,4}

Supplementary Tables and Figures:

Table S1. Vietnam gastritis patient demographics

Histologic diagnosis	N	<i>H. pylori</i>	Active <i>H.</i>	Mean age (\pm) SD	Gender (% male)
		IgG (% positive)	<i>pylori</i> (% positive)		
G w/o HP	27	52	0	41 (13)	59
G w/ HP	30	97	100	45 (14)	77
Atrophy	31	100	93	47 (15)	74
IM +Atrophy	27	100	93	54 (12)	52

Table S2. Chinese gastric cancer patient demographics

Histologic diagnosis	N	Lymphatic metastasis	Mean age (\pm) SD	Gender (% male)
		(% positive)		
Control	21	0	58 (10)	52
Adenocarcinoma	47	18	51 (10)	53
Well-differentiated	10	20	56 (10)	70
Moderately-differentiated	21	14	53 (8)	71
Poorly-differentiated	16	19	48 (10)	44
Mucinous adenocarcinoma	4	25	50 (9)	75.
Signet ring cell carcinoma	12	25	45 (14)	67

Table S3. Primers used for quantitative PCR ($T_m = 65^\circ\text{C}$ for all primers)

Genes	Forward Sequence	Reverse Sequence
Slfn4	5'GCCCTCTGTTCAAGTCAAGTGCC3'	5' CCCAGATGAAATCCTTTCCACGA3'
hSLFN12L	5'TTGACCGAGAAGGAATGGAT3'	5'GCAGAAGGTTTTTGGAGCAC3'
Arg1	5' AACACGGCAGTGGCTTTAAC3'	5' GGTTTTCATGTGGCGCATT3'
Nos2	5' CGAAACGCTTCACTTCCAA3'	5' TGAGCCTATATTGCTGTGGCT3'
p65	5'CTTCTCAGCCATGGTACCTCT3'	5'CAAGTCTTCATCAGCATCAAAGT3'
Tnf	5'ATAGCTCCCAGAAAAGCAAGC3'	5'CACCCCGAAGTTCAGTAGACA3'
IL1a	5'GGAGAAGACCAGCCGTGTTGCT3'	5'CCGTGCCAGGTGCACCCGACTT3'
Csf-1	5'AAGGGACTCACTAGCCTGGA3'	5'ATCAGGCTCTCTTCTTGGGA3'
Csf-2	5'GCCATCAAAGAAGCCCTGAA3'	5'GCGGGTCTGCACACATGTTA3'
Cyld	5'TGCCTTCCAACCTCTCGTCTTG3'	5'AATCCGCTCTTCCCAGTAGG3'
Runx3	5'GGTTCACGACCTTCGATT3'	5'CGGTGGTAGGTAGCCACTTG3'
Cebpe	5'GCTACAATCCCCTGCAGTACC3'	5'TGCCTTCTTGCCCTTGTG3'
Cebpb	5'GGTTTCGGGACTTGATGCA3'	5'CAACAACCCCGCAGGAAC3'
Trp53INP1	5'CTTCTCCTGTTTACCTGCATCTT3'	5'TGATAGTGGTTAATCCACCTGCT3'
Traf2	5'ACTTCACCAGAAAGCGTCAG3'	5'GGTTTTCTCTGTAGGTCTTCCG3'
Cxcl5	5'CTCAGTCATAGCCGCAACCGAGC3'	5'CGCTTCTTCCACTGCGAGTGC3'
Pten	5'TGGGGAAGTAAGGACCAGAG3'	5'GGCAGACCACAACTGAGGA3'
Clusterin	5'CTGTCCACTCAAGGGAGTAGG3'	5'GTGTCCTCCAGAGCATCCTC3'
Tff2	5'CTTGGCCCTGACCTGTATGT3'	5'TAG GTT GCT CAG GTG TCA CG 3'
Gif	5'CCCTCTACCTCCTAAGTGTCTC3'	5'CTGAGTCAGTCACCGAGTTCT3'
130b-BS1	5'CACCCATCCATGGTTGAGC3'	5'GGAGTGGGAGGTGAGGGTTA3'
130b-BS2	5'TTCTCCTCCACCTCAATCCG3'	5'CCCACCACCCCAATACA3'
130b-BS3	5'GCCACCACGTCCAAATA3'	5'GCCGAGACCCTGTGGAAA3'
IKB Promoter	5'GACGACCCCAATTCAAATC3'	5'TCAGGCTCGGGGAATTTCC3'
NOS-BS1	5'CCACCCTTGATACCGCAT3'	5'CTCCACTCCTACCCATTCT3'
NOS-BS2	5'GGACTTGGGACCAGAAAGAGGTG3'	5'GCCATCCAGAGAGTTGTTTTGC3'

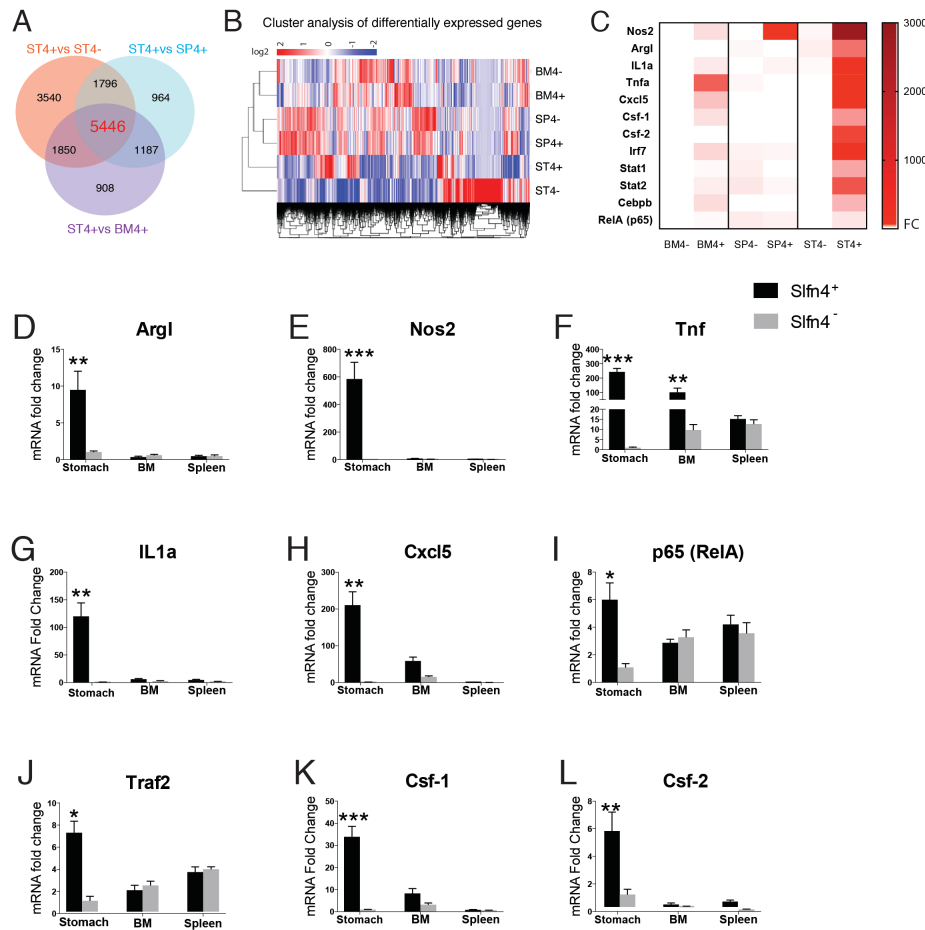


Figure S1. RNAseq analysis of SLFN4⁺ cells and validation by qPCR. WT chimeric mice reconstituted with Slfn4-tdT bone marrow were treated with Tx 2 weeks prior to euthanization. Slfn4⁺ vs SLfn4⁻ cells sorted from stomach (ST4^{+/-}), spleen (SP4^{+/-}) and bone marrow (BM4^{+/-}) were profiled by RNAseq and miRNA NanoString nCounter Technology. A) A Venn diagram displaying the number of differentially-expressed genes determined with RNA-seq in each group and the overlap between groups. B) Cluster analysis of differentially-expressed genes related to MDSCs. C) Heatmap for several differentially-expressed genes. D-L) The expression of 9 genes was analyzed by qPCR to validate RNAseq results. N=3 expts. One-way ANOVA followed by Tukey's multiple comparisons test on log-transformed values. P values are relative to SLFN4⁻ in each tissue group. *P<0.05, **P<0.01, ***P<0.001. Median and interquartile range.

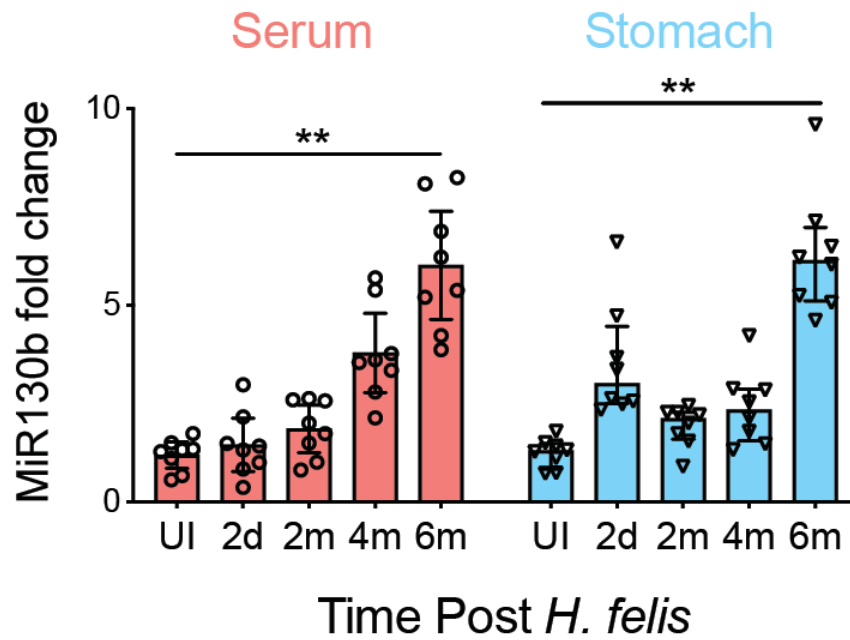


Figure S2. MiR130b expression in serum and stomach tissue determined by qPCR after *H. felis* infection over 6 months. N=8 mice per time point over 3 expts.

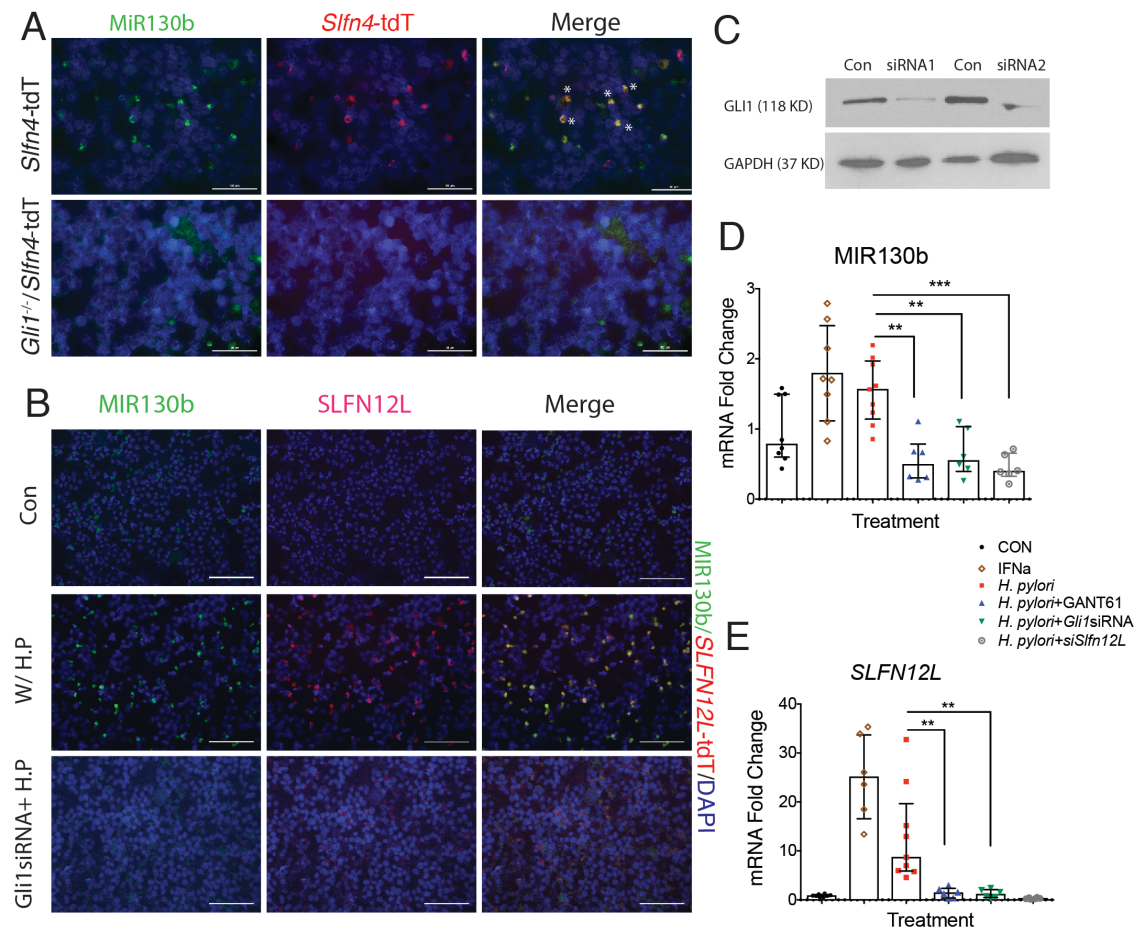


Figure S3. GLI1 regulates co-localization of MIR130b with SLFN4/SLFN12L expression. FISH for MiR130b (green) followed by immunofluorescent staining for SLFN4 (red) was performed in A) thioglycollate-elicited peritoneal cells collected from *Sfn4-tdT* mice or *Gli1^{-/-}/Sfn4-tdT* mice treated with IFN α for 24h. Asterisks indicate co-localization. N=3 mice per group. and in B) HL-60 cells treated with scrambled siRNA w/o (Con), w/ *H. pylori*, or *Gli1*siRNA with *H. pylori*. N=5 expts. Scale bar= 50 μ m. C) Knockdown efficiency of *Gli1* siRNAs was validated by Western blot analysis. GAPDH as a loading control. D) MIR130b and E) *SLFN12L* expression determined by qRT-PCR after treating HL-60 cells with IFN α (800U/ml), *H. pylori* (MOI of 10), GANT61 (10 μ m), *GLI1* or *SLFN12L* siRNA (100nM) or recombinant SHH (200 ng/ml) in the medium for 24 to 48h. N=6–9 expts. One-way ANOVA followed by Tukey's multiple comparisons test on log-transformed values was performed. P values are relative to Con. **P<0.01. Horizontal lines represent the median and interquartile range.

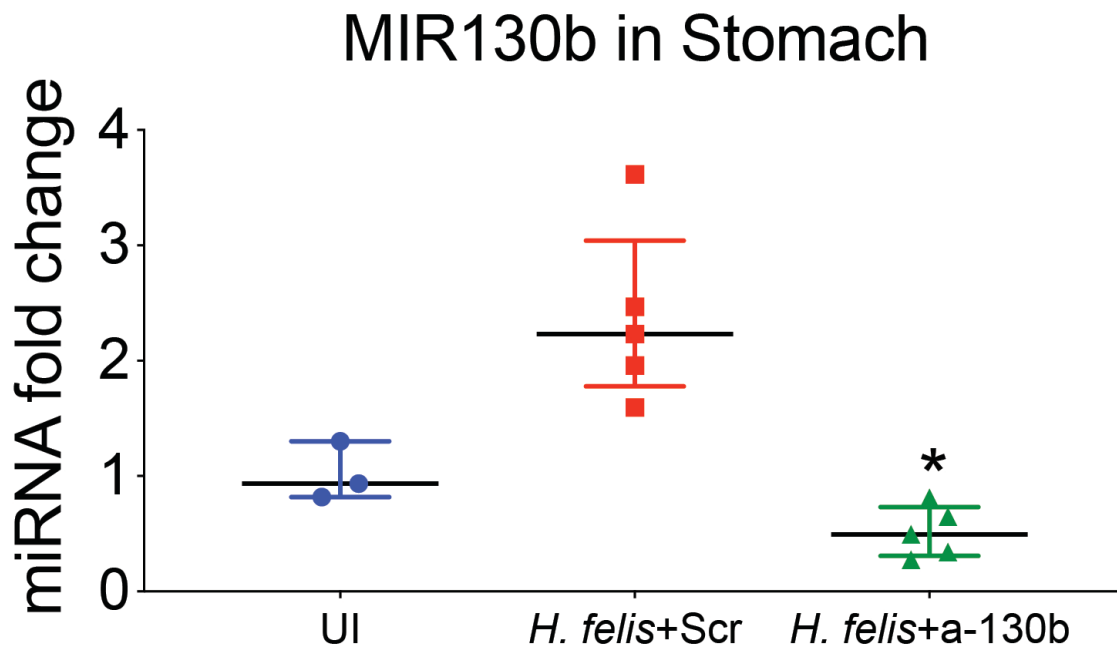


Figure S4. Q-PCR analysis of MiR130b in mouse stomachs 3 weeks after in vivo transfection. Mice infected with *H. felis* for 4 months were treated with antisense MIR130b (a-130b) or scrambled control (Scr) using Invivojectamine. Three weeks post injection, mice were necropsied and mRNA was extracted from the corpus. MiR130b expression was analyzed by qPCR. Horizontal lines represent the median and interquartile range. One-way ANOVA followed by Tukey's multiple comparisons test on log-transformed values. Samples were collected over N=3 expts. *P<0.05 for a-130b treated compared to scrambled control.

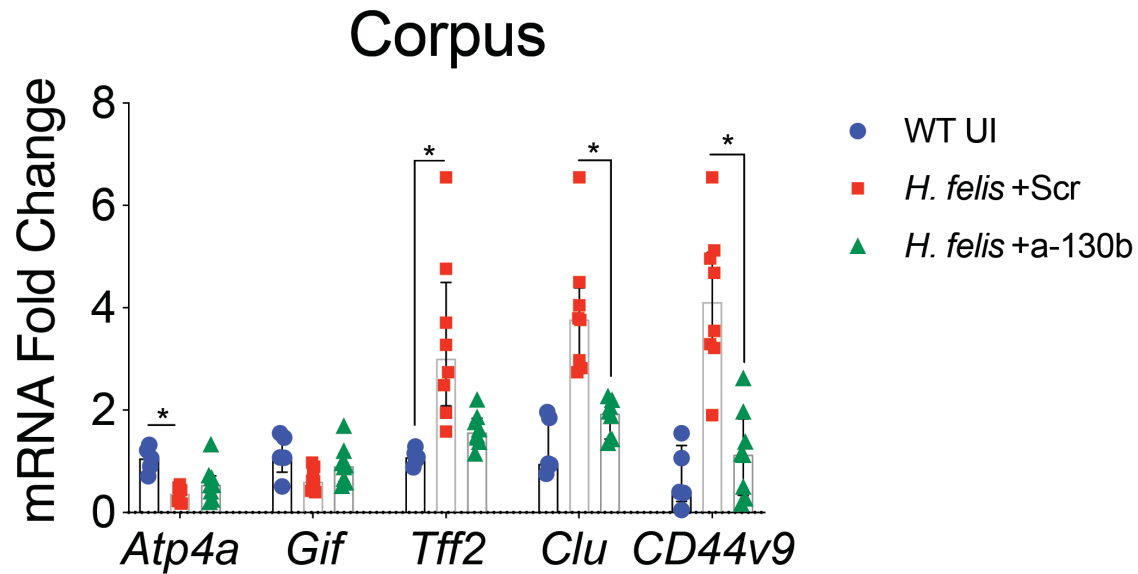


Figure S5. Q-PCR analysis of SPEM markers. Mice infected with *H. felis* for 4 months were treated with antisense MIR130b (a-130b) or scrambled control (Scr) using Invivofectamine. Three weeks post injection, mice were necropsied and mRNA was extracted from the corpus. *ATP4 α* , Gastric intrinsic factor (*GIF*), *Tff2*, Clusterin (*Clu*) and *CD44v9* mRNA were analyzed by qPCR. Horizontal lines represent the median and interquartile range. N=5 mice in WT UI group and N=8 mice in the oligo-treated groups over 3 expts. One-way ANOVA followed by Tukey's multiple comparisons test on log-transformed values. Wildtype uninfected (WT UI). *P<0.05.

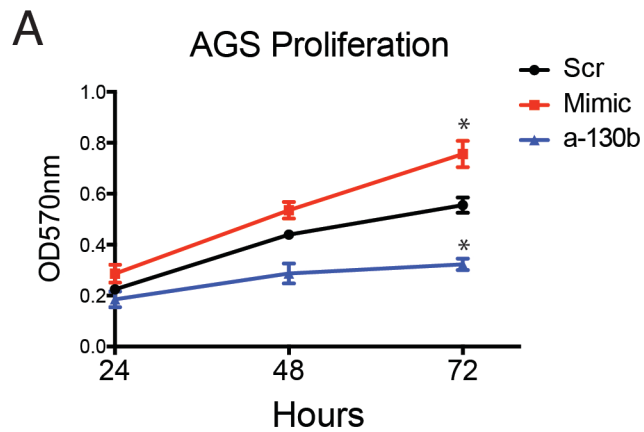


Figure S6. MIR130b promotes AGS cell proliferation. AGS cells were transfected with MIR130b mimic, antisense MIR130b (a-130b) or scrambled control (Scr). The MTT proliferation assay was performed at different time points. Absorbance was measured at 570nm. One-way ANOVA followed by Tukey's multiple comparisons test on log-transformed values. *P-values are relative to Scr. *P<0.05 for N=4 expts. Horizontal lines represent the median and interquartile range.

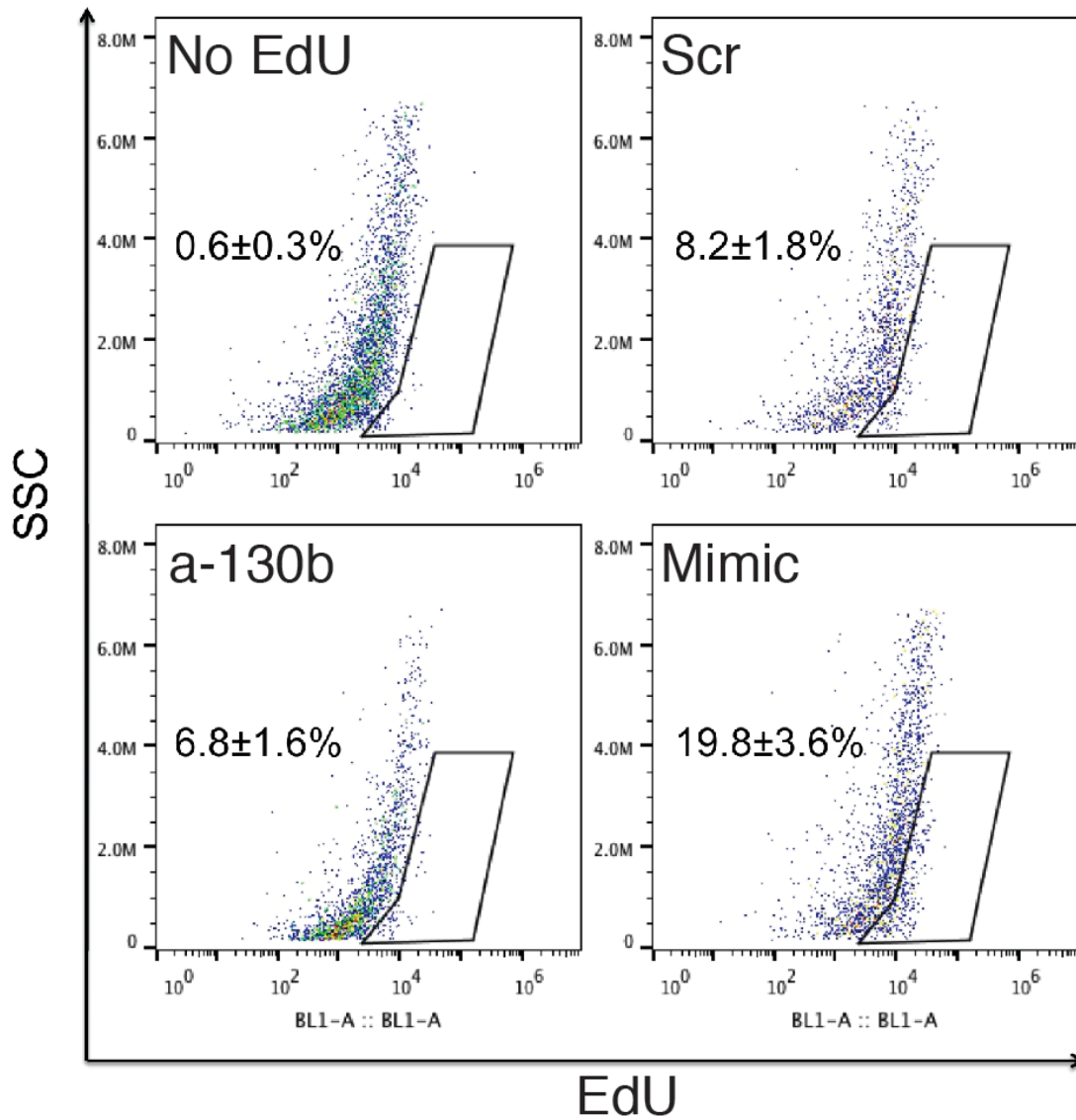


Figure S7. MIR130b promotes normal human gastric organoid

proliferation. Normal human gastric organoids were transfected with MIR130b mimic, antisense (a-130b) or scrambled control (Scr). Single cells from dissociated organoids were labeled with EdU. Proliferation were determined by flow cytometry. N=4 expts. The median ± interquartile range.

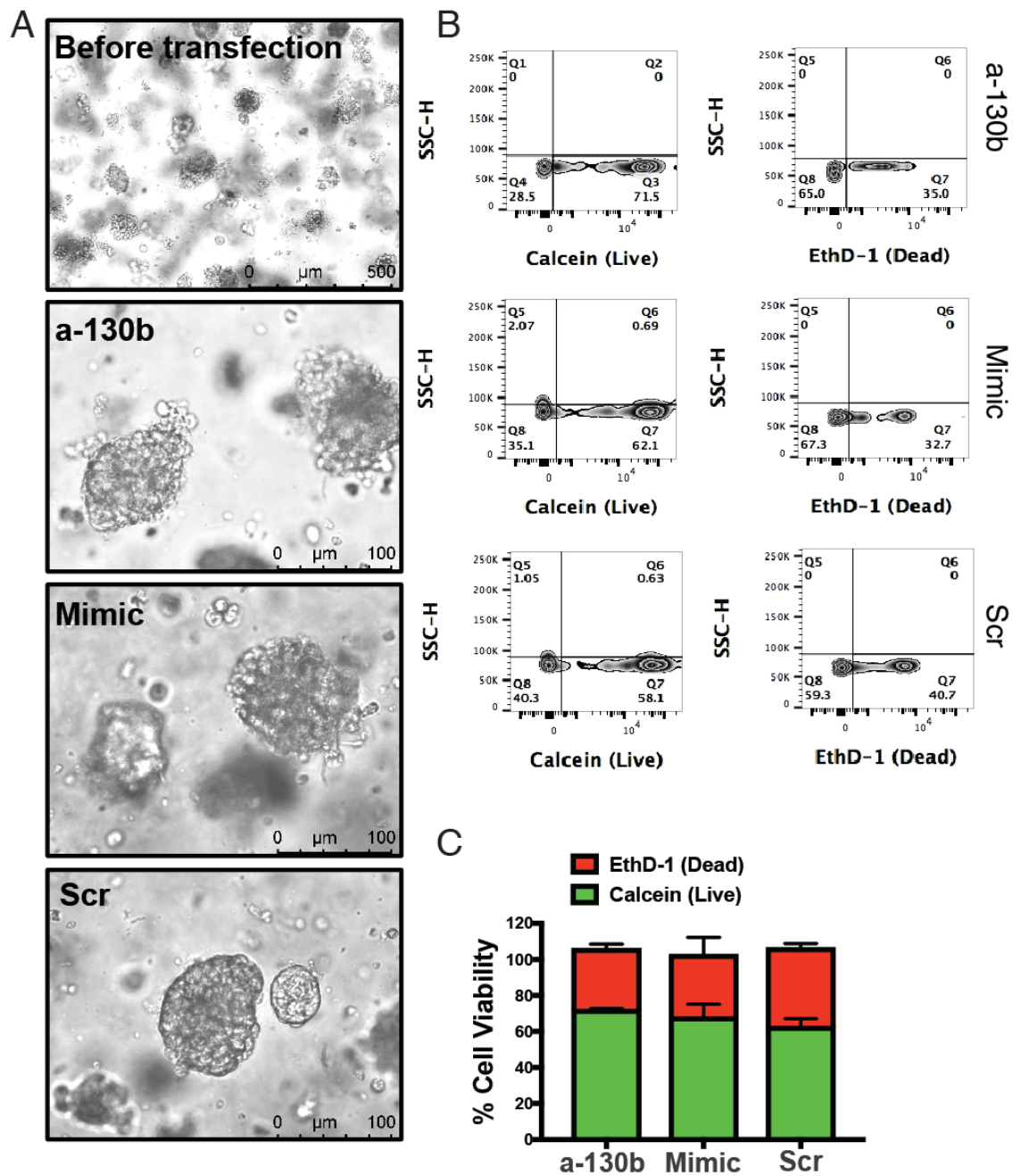
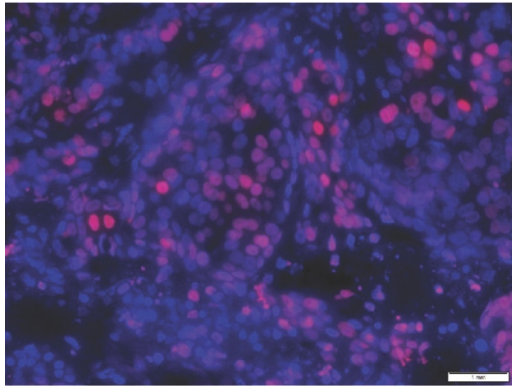


Figure S8. Organoid viability after transfection of mimic/antisense/Scr MIR130b sequence. A) Morphology of human gastric cancer organoids transfected with MIR130b Mimic, antisense (a-130b) or scrambled (Scr) oligos prior to xenograft transplantation. B) The cell viability was determined for each group by flow cytometry and summarized in the stacked bar graph C).



Human histone 3/DAPI

Figure S9. Human histone 3 in xenograft. The mouse xenograft tissues were stained with human histone H3 to confirm engraftment of the human gastric cancer organoids. Shown is a representative image of the staining at Mag 200X.

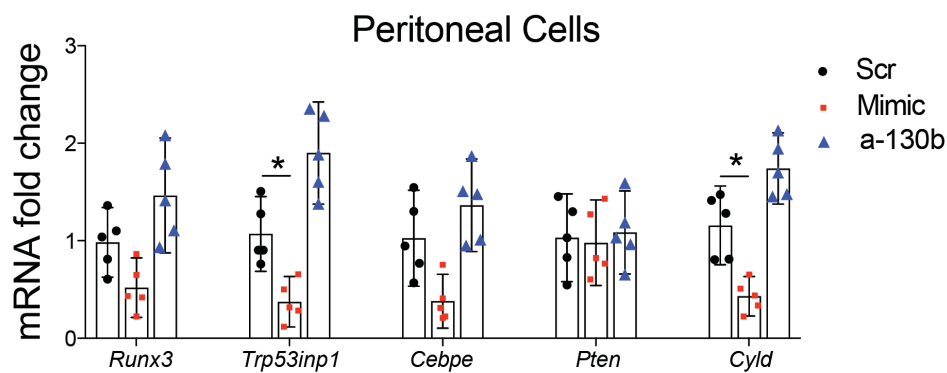


Figure S10. Validation of MiR130b targets in peritoneal cells by qPCR. Shown is the median and interquartile range for N=5 expts. One-way ANOVA followed by Tukey's multiple comparisons test on log-transformed values was used. *P<0.05.

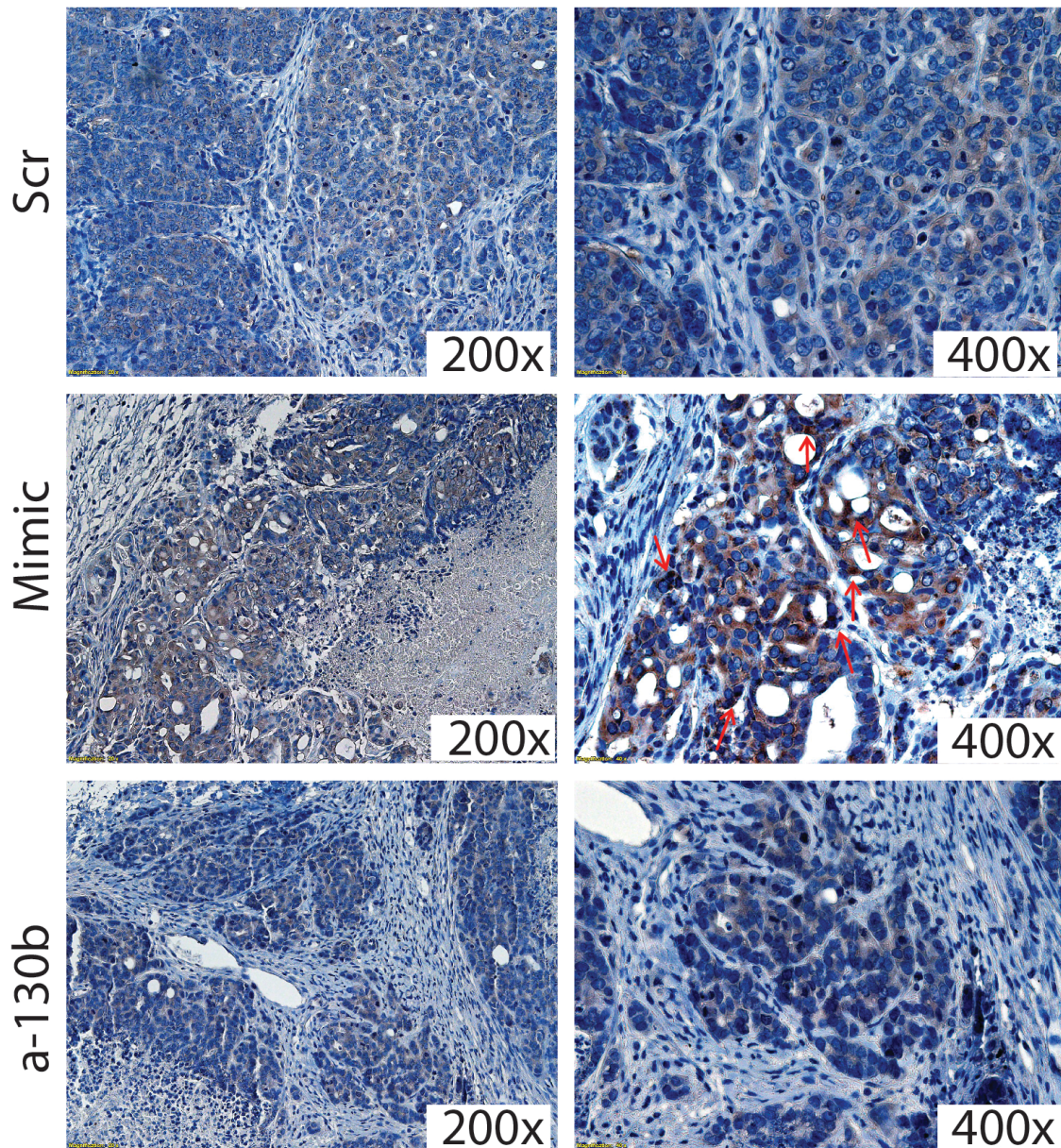


Figure S11. IHC staining of NFκb p65 subunit in representative xenograft tumors from each treatment group at a magnification of 200X and 400X. Arrows indicate positively stained nuclei.

References:

1. Kim D, Pertea G, Trapnell C, et al. TopHat2: accurate alignment of transcriptomes in the presence of insertions, deletions and gene fusions. *Genome Biol* 2013;14(4):R36. doi: 10.1186/gb-2013-14-4-r36 [published Online First: 2013/04/27]
2. Cui X, Kong C, Zhu Y, et al. miR-130b, an onco-miRNA in bladder cancer, is directly regulated by NF-kappaB and sustains NF-kappaB activation by decreasing Cylindromatosis expression. *Oncotarget* 2016;7(30):48547-61. doi: 10.18632/oncotarget.10423 [published Online First: 2016/07/09]
3. Fort RS, Matho C, Oliveira-Rizzo C, et al. An integrated view of the role of miR-130b/301b miRNA cluster in prostate cancer. *Exp Hematol Oncol* 2018;7:10. doi: 10.1186/s40164-018-0102-0 [published Online First: 2018/05/11]
4. Asanoma K, Hori E, Yoshida S, et al. Mutual suppression between BHLHE40/BHLHE41 and the MIR301B-MIR130B cluster is involved in epithelial-to-mesenchymal transition of endometrial cancer cells. *Oncotarget* 2019;10(45):4640-54. doi: 10.18632/oncotarget.27061 [published Online First: 2019/08/07]